# Cr Dopant Effect on MgO Thin Film Structural, Optical and Morphology Properties

Ahmet TAŞER[1*] , Muhammed Emin GÜLDÜREN[2] , Harun GÜNEY[3]

[1]Patnos Vocational School, Departments of Medical Services and Techniques,
Agri Ibrahim Cecen University, Agrı – Turkey
[2]Vocational School, Department of Electric and Energy, Agri Ibrahim Cecen University, Agrı - Turkey
[3]Hınıs Vocational School, Departments of Medical Services and Techniques,
Atatürk University, Erzurum-Turkey

**Abstract**

Cr dopant effect is investigated on MgO thin films which are grown by using successive ionic layer adsorption reaction (SILAR) technique. UV-Vis spectroscopy, XRD (X-ray diffraction), SEM (scanning electron microscope) measurements are performed to determine how Cr doping alters morphological, structural and optical properties of MgO nanostructures. UV-Vis spectroscopy measurements of plain MgO thin films and Cr added MgO thin films have shown that bandgap decreased with rising Cr additive from 4.00 eV to 3.45 eV. XRD measurements of samples have shown that all thin films were cubic structures and have planes of (200), and (220). The surface morphologies have presented that both pure MgO nanostructures and Cr added MgO nanostructures have nanowall formations and Cr dopant changed surface of MgO.

**Keywords:** MgO thin films, SILAR method, Cr doped, Uv-Vis spectroscopy, XRD, SEM.

## Cr Katkısının MgO İnce Filmin Yapısal, Optik ve Morfolojik Özelliklerinin Üzerine Etkisi

**Öz**

Ardışık iyonik tabaka adsorpsiyon reaksiyonu (SILAR) yöntemi ile üretilen MgO ince filmleri üzerinde Cr katkı maddesinin etkisi araştırıldı. Cr katkı maddesinin MgO ince filmler üzerindeki etkisi UV-Vis spektroskopisi, XRD (X-ışını kırınımı), SEM (taramalı elektron mikroskobu) ölçümleri ile optik, yapısal ve morfolojik özellikleri araştırılmıştır. Katkısız ve Cr katkılı MgO ince filmlerin UV-Vis spektroskopi ölçümleri, Cr katkı maddesinin yükselmesine bağlı olarak, MgO nano yapılarının bant aralığının 4.00 eV'den 3.45 eV'a kadar azaldığı gösterilmiştir. Numunelerin XRD ölçümleri, numunelerin kübik yapılar olduğunu ve (200) ve (220) kristal yapı düzenlerine sahip olduklarını göstermiştir. Yüzey morfolojileri, hem MgO hem de Cr katkılı MgO ince filmlerinin nanowall yapılarına sahip olduğu ve MgO nano yapılarının yüzey şekilleri Cr katkısı dolayısıyla değiştiği gösterilmiştir.

**Anahtar Kelimeler:** MgO ince filmler, SILAR metodu, Cr katkısı, Uv-Vis spektroskopisi, XRD, SEM.

*Corresponding Author: ataser@agri.edu.tr

## 1. Introduction

Magnesium oxide (MgO) is a highly insulating material whose bulk wide-band gap is around 7 eV. However, nanostructure MgO bandgaps can be found as low as 5eV (Yu, 2018). The crystal structure of MgO is as same as that of NaCl with remarkable features such as chemical inertness, low electron affinity, optical transparency, good heat resistance and mechanical durability, and efficient thermal conductors. MgO is often preferred in theoretical and practical research areas. Magnesium oxide has been employed in various industrial applications as heat resistant, plasma display panels, liquid crystal screens, electron emitter, ionized mass spectrometers and fluorescent display tubes (Raoand Sunandana, 2008). In addition to that it is proven that MgO nanocrystals highly effective as absorbers for hazardous chemicals such as poisonous gases. Metal oxide thin films can be fabricated by using diverse techniques such as ion beam sputtering (Liu at al., 2015), reactive magnetron sputtering (Qi et al., 2017), plasma enhanced metal organic chemical vapor deposition (Li et al., 2012), and physical vapor deposition (Eiji et al., 1997). SILAR method has been used in this work. This method has advantages such as high deposition rate in certain time periods, cost-effectiveness and sufficient deposition of specific atoms. Magnesium oxide emits at different wavelengths with various energy states. Modifications in characteristics of MgO can be formed with help of various additives. Material properties can be adjusted according to needs. For example, the devices which are made of MgO and doped MgO have become very common in display technology (Jung et al., 2014; Visweswaran et al., 2020). Effect of doping has found to be a potent way to alter essential structure of oxide materials as well as their electronic form and chemical organization. This approach depends on the capability of the doped atoms to swap electrons with host materials. To investigate the effect of Cr doping on magnesium oxide thin films, the untouched and Cr added MgO nanostructures were fabricated by using SILAR technique. These thin films have been characterized optically, structurally and morphologically at different doping values.

As we mentioned before, there are many studies in the literature regarding the production of MgO thin films (Valanarasu et al., 2014; Płóciennik et al., 2016; Idris et al., 2019). In these studies, the use of the SILAR technique as a production technique is almost nonexistent, which has caused a low cost technique such as the SILAR technique to be left behind. In this study, we wanted to show that MgO thin films can be produced with the SILAR technique. Also, these thin films can be grown successfully with various other dopants and shed light on new studies. Thus, it can be possible to produce undoped MgO and doped MgO thin films with less cost for application areas.

## 2. Materials and Methods

### 2.1 Materials

Magnesium nitrate hexahydrate (Mg $(NO_3)_2$ +$6H_2O$), chromium nitrate (Cr $(NO_3)_3$), Sulfuric acid ($H_2SO_4$) and Ammonium hydroxide solution ($NH_4OH$) were purchased from SigmaAldrich and all were 99.99% pure.

### 2.2 Synthesis of MgO thin films

Deposition of high quality thin films depend on substrate cleaning. The cleanliness of the glass substrates is a crucial part of fabrication process due to contaminated substrate surfaces prevent producing homogeneous

films and lead undesirable or non-existent nucleation areas. First step of sanitation starts with bathing prepared glass slides in an ultrasonic cleaner. The glass slides are soaked in sulphuric acid whose concentrations degraded using DI water by the ratio of 1/5 and bathed for 5 minutes in the ultrasonic cleaner. Then, same process repeated by submerging the glass slides into deionized water (DI water) instead of sulphuric acid and also cleaned ultrasonically for 5 minutes. Soda lime glass substrates are used to grow the pure and Cr added magnesium oxide nanostructures. The SILAR method is employed to perform deposition on these glass slides. This approach employs cationic and anionic precursors. Thus, the binary and ternary blend of semiconductors can be executed by using the SILAR method. During the experiments, 0.1 molar (M) magnesium nitrate $(Mg(NO_3)_2 + 6H_2O)$ and different molar ratios of 0.1 M chromium nitrate $(Cr(NO_3)_3)$ are chosen to be the cationic precursor. 0.5%, 1%, 2%, and 4% of 0.1M $Cr(NO_3)_3$ are used as doping agents. The anionic precursor is DI water which maintained at 90 °C. The pH level of the anionic solution is set to 11.5 with the help of ammonium hydroxide (29%) solution. Afterwards, the substrates are first dipped into the cationic solution for 30 seconds and then into the anionic solution for 30 seconds. All steps are run for 30 cycles. After the deposition, the pure and Cr added MgO nanostructures are air dried and finally annealed in atmospheric air at 400 °C temperature for 60 minutes.

*2.3 Characterization techniques of MgO thin film*

**UV-vis:** Ultraviolet and Visible Region optical transmission spectroscopy technique is used to determine the forbidden energy range of thin films produced. It is a device used to determine how much of the light with different wavelengths sent from the light source passes through the material and how much is absorbed by the material.

**XRD:** The characteristic X-ray obtained by impacting the accelerated electron beam on the copper plate is sent on the thin film and the reflected or diffracted rays are recorded with the help of the detector. It is a technique used to determine the structural and chemical properties of thin films by examining the diffraction pattern formed specific to the crystal structure.

**SEM:** SEM technique is used to examine the surface morphology of thin films produced. Image in Scanning Electron Microscope; High voltage accelerated electrons should be focused on the sample. This electron beam should be scanned on the sample surface. The effects that occur as a result of the interference between the electron and the sample atoms during scanning should be collected in suitable sensors. Finally, it is achieved by transferring this information to the screen of a cathode ray tube after passing through signal amplifiers.

**EDX:** It is a method used to describe the elemental composition on any sample or sample. It is a technique used in scanning electron microscopy. The analysis process is performed by sending a scanning electron beam on the sample.

## 3. Research Findings

### 3.1 Absorption analysis

The absorption datas are evaluated to examine the results of Cr doping on the optical properties MgO nanostructures. The UV–vis spectrum of all samples are computed in the

domain of 300 to 800 nm. in figure 1 displays absorbance measurements for pure MgO thin films and $Cr^{3+}$ doped magnesium oxide nanostructures. The absorption values increased with Cr doping for the entire wavelength range. Wide absorption areas in the visible light scope might be achieved as a result of an exchange which can occur in the conduction band electrons (sp-d) and d electrons of the $Cr^{3+}$. Thus, electrons of the $Cr^{3+}$ displace $Mg^{2+}$ electrons (Xu et al., 2010). The electron transfers between s–d and p–d states initiate the adjustment in the conduction band. These alterations can be either negative or positive. As a result of this incident, the valence band forms independently from the conduction band and strong absorption occurs at Cr-doped MgO thin films (Jayanthi et al., 2010). These absorption bands vary with changing in the concentration of $Cr^{3+}$ ions, as seen in the figure 1.
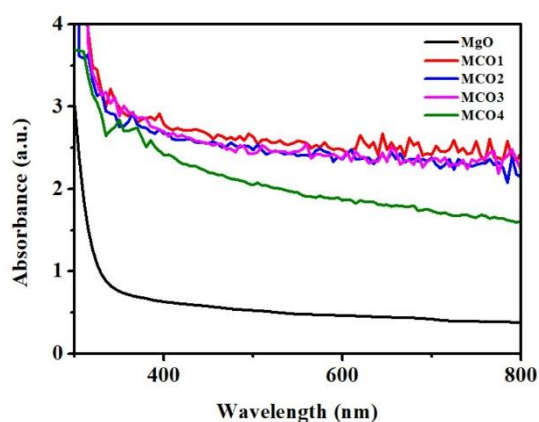


**Figure 1.** The absorbance graph of pure MgO and MgO:Cr thin films with different Cr doping concentrations.

The computed energy band gap (Eg) of untouched MgO and Cr added MgO nanostructures are presented in figure 2. As a result of the Cr doping, the computed energy band gap of MgO nanostructures is reduced. Therefore, The Moss-Burstein effect can be applied here to clarify this incident (Khan et

al., 2014). The Eg values for semiconductors were determined using mathematical formulas (1) and (2). These equations are as follows:

$$\alpha = \frac{Absorbance}{t} \qquad (1)$$

$$(\alpha h\nu) = B\left(h\nu - E_g\right)^{1/2} \qquad (2)$$

In equations (1) and (2), α refers to a measure for absorption, t used to quantify thickness, and hν refers to the photon energy. Also, Eg is the optical bandgap and B is an invariable. It is found that the Eg for virgin magnesium oxide has been computed as 4 eV. This quantity is deviated from 4eV to 3.45 eV as a result of adding 4% Cr to pure MgO. These values can be compared with band gap values cited in the literature (Kadari et al., 2016). The calculated values of the band gap energies are given in a table in the figure 2. From these results, it is clear that the shift in the band gap of nanoparticle is due to the quantum confinement. This shift is also due to the introduction of chromium ions ($Cr^{3+}$) in MgO lattice.
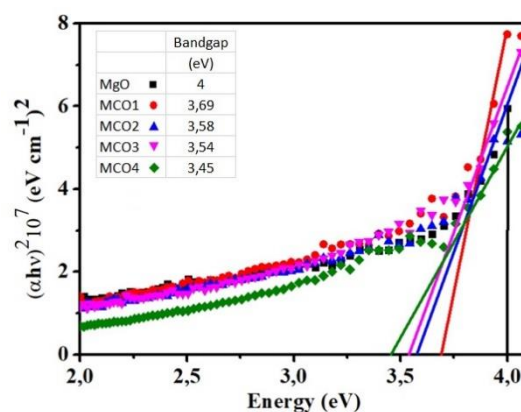


**Figure 2.** Band gap variation of untouched and 0.5%, 1%, 2%, 4% Cr added MgO

## 3.2 XRD analysis

X-ray diffraction (XRD) spectrum of pure and Cr added MgO nanostructures are given in figure 3. It was determined from data of ICSD card number 00-45-0946 that nanostructures of MgO have (002) and (220) oriented peaks and cubic structure. It was seen that these results are compatible with the literature (Mishra et al., 2013; Maiti et al., 2017; Güney and İskenderoğlu, 2018;Caiet al., 2017).

No different phase was observed from XRD spectra such as pure Cr or CrO. From this result, we can say that Cr doping does not disrupt the crystal structure of MgO films, unlike, it improves the crystallinity of the films by providing a good placement in the mesh.

Table 1 shows the lattice calculations of XRD spectrum peaks for the pure and Cr added MgO nanostructures. The Debye-Scherrer formula, Eq. (3), is applied to determine the average particle size (D) of thin films, and full width at half maximum (FWHM) of XRD as shown in Table 1.

$$D = \frac{0.94\lambda}{\beta cos\theta} \tag{3}$$

$\lambda$ refers to the wavelength of X-rays, the full width at the maximum half of the peak is given with $\beta$, and $\theta$ represents Bragg angle. It was observed that D values changed with the doping of thin films. This situation shows that the Cr ions contributed to replace Mg atoms in the MgO film structure (Aksay, 2019;Shkir et al., 2020).

For thin films, the volume of the unit cell (V) and the lattice constant (a) are calculated from XRD spectra data using the Eqs. (4) and (5).

$$d = \frac{a}{\sqrt{(h^2+k^2+l^2)}} \tag{4}$$

$$V = a^3 \tag{5}$$

The changes in the calculated volume (V) and lattice constant (a) values of pure MgO and Cr doped MgO nanostructures are given in Table 1. It was observed that the a and V values calculated for MgO thin films are compatible with the values of a = 4.2112 Å and V = 74.68 Å$^3$ for MgO cubic structures with ICSD standard card number 00-45-0946.

**Table 1.** Lattice calculations of XRD spectrum peaks for pure and Cr added MgO nanostructures

| Sample Name | hkl | $E_g$ (eV) | Pos. (°2θ) | Height (cts) | FWHM (°2θ) | d-spacing (Å) | I (%) | $I/I_0$ | D (nm) | $D_{avg.}$ (nm) | a (Å) | V (Å)$^3$ |
|---|---|---|---|---|---|---|---|---|---|---|---|---|
| MgO | (002) | 4.00 | 42.81 | 276 | 1.8464 | 2.10936 | 100 | 1 | 9.41 | 12.47 | 4.2187 | 75.0831 |
|  | (220) |  | 61.79 | 174 | 1.0760 | 1.49275 | 63 | 1.62 | 15.52 |  |  |  |
| MCO1 | (002) | 3.69 | 42.82 | 62 | 1.6398 | 2.11199 | 100 | 1 | 10.57 | 11.94 | 4.2240 | 75.3643 |
|  | (220) |  | 61.69 | 32 | 1.2912 | 1.50353 | 51 | 1.31 | 13.31 |  |  |  |
| MCO2 | (002) | 3.58 | 42.69 | 582 | 1.8044 | 2.11794 | 100 | 1 | 10.04 | 9.57 | 4.2359 | 76.0030 |
|  | (220) |  | 61.76 | 298 | 1.8506 | 1.50212 | 51 | 1.31 | 9.10 |  |  |  |
| MCO3 | (002) | 3.54 | 42.54 | 482 | 1.7334 | 2.12501 | 100 | 1 | 11.11 | 10.81 | 4.2500 | 76.7667 |
|  | (220) |  | 61.65 | 230 | 1.6613 | 1.50456 | 48 | 1.22 | 10.51 |  |  |  |
| MCO4 | (002) | 3.45 | 42.42 | 370 | 1.8316 | 2.13094 | 100 | 1 | 11.14 | 9.64 | 4.2619 | 77.4112 |
|  | (220) |  | 61.94 | 227 | 1.9712 | 1.49824 | 61 | 1.57 | 8.15 |  |  |  |
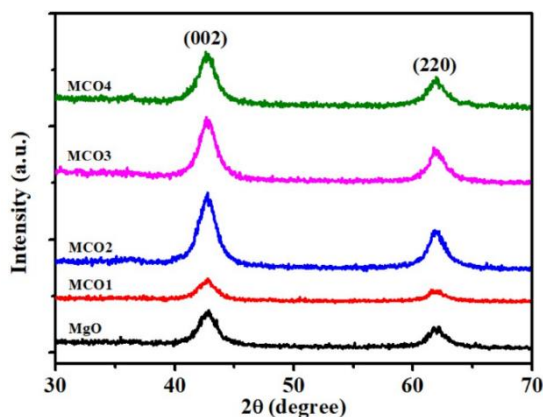
**Figure 3.** X-ray diffraction (XRD) spectra of pure and Cr added MgO nanostructures
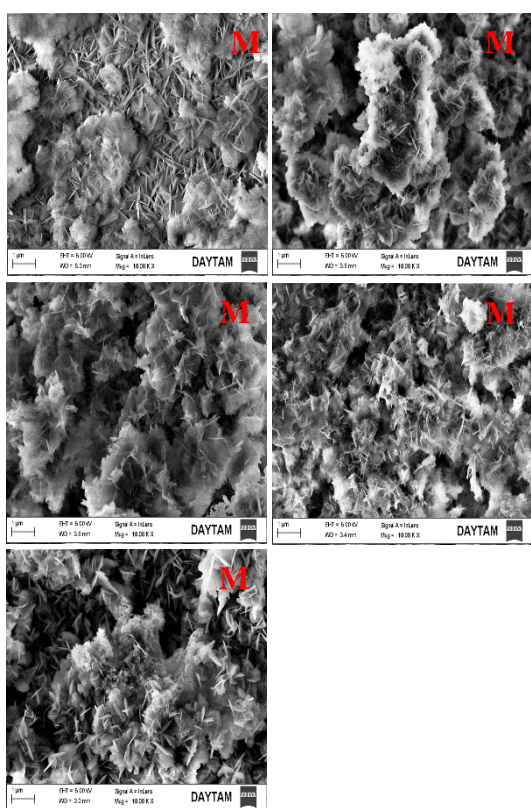


**Figure 4.** SEM images of pure and Cr added MgO nanostructures

### 3.3 SEM analysis

In figure 4, magnified 10,000 times SEM images of MgO and Cr doped MgO thin films are illustrated to examine surface morphologies and to observe how Cr dopant has an effect on the surface of MgO samples. As can be seen in the figure 4, both MgO and

Cr doped MgO samples have a nanowall structure. However, changes in the density and homogeneity of the nanowall structures of the samples with the Cr dopant are observed.

EDAX measurements were conducted to determine the chemical contents of the produced thin films as shown in figure 5. The EDAX spectra of the produced thin films unveiled the presence of magnesium, chromium and oxygen elements. And the results were tabulated within the figure 5 as atomic percentages of these elements. Therefore, the EDAX analysis confirmed the presence of Cr in the produced MgO nanostructures.
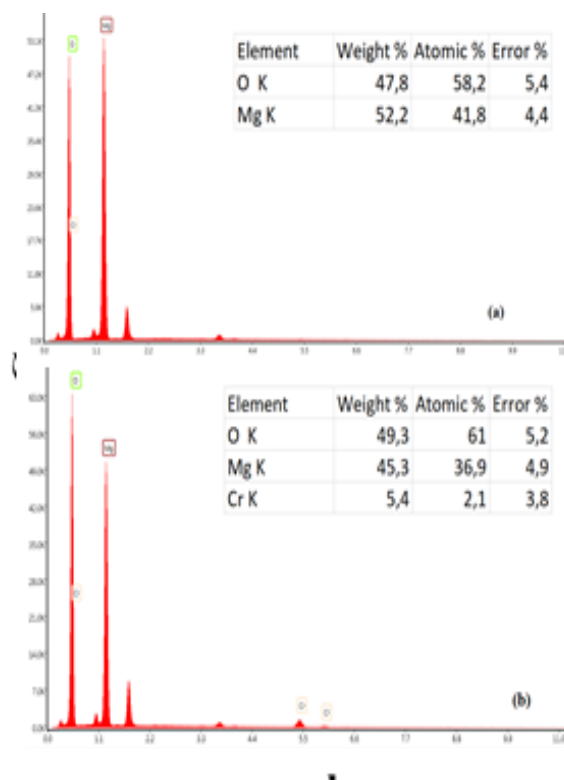


| Element | Weight % | Atomic % | Error % |
|---------|----------|----------|---------|
| O K | 47,8 | 58,2 | 5,4 |
| Mg K | 52,2 | 41,8 | 4,4 |

(a)

| Element | Weight % | Atomic % | Error % |
|---------|----------|----------|---------|
| O K | 49,3 | 61 | 5,2 |
| Mg K | 45,3 | 36,9 | 4,9 |
| Cr K | 5,4 | 2,1 | 3,8 |

(b)

**Figure 5.** EDAX and element contents and quantities of a) undoped and b) Cr doped MgO thin films

## 4. Results

In this work, the effect of Cr doping on MgO thin films that are fabricated by using the

SILAR method has been observed. Both pure and Cr doped MgO nanostructures have the cubic structure. The bandgaps of samples decreased by Cr dopant. The morphology of MgO was significantly changed by Cr dopant. It is also noted that the band gaps of MgO nanostructures can be tuned by introducing Cr ions to these structures. Hence, optical instruments technology can benefit from these thin films.

## Acknowledgement

## 5.  References

Aksay S. 2019. "Effects of Al dopant on XRD, FT-IR and UV–vis properties of MgO films", Physica B: Condensed Matter, 50, 280-284.

Cai, Y., Wu, D., Zhu, X., Wang, W., Tan, F., Chen, J., Qiao, X. and Qiu, X. 2017. "Sol-gel preparation of Ag-doped MgO nanoparticles with high efficiency for bacterial inactivation", Ceram. Int., 43, 1066.

Eiji, F., Tomozawa, A., Fujii, S., Torii, H., Takayama, R. and T. Hirao. 1997. "Crystallographic Orientations of MgO Films Prepared by Plasma-Enhanced Metalorganic Chemical Vapor Deposition" Japanese journal of applied physics, 33 (11), 6331

Güney, H. and İskenderoğlu, D. 2018. "The effect of Ag dopant on MgO nanocrystallites grown by SILAR method", Mater. Sci. Semicond. Process, 84, 151.

Idris, M. S., Subramani, S., Wan Ahmad Kamil, W. M., & Devarajan, M. (2019). Synthesis of MgO Thin Film on Aluminum and Copper Substrates as Thermal Interface Materials. IEEE Transactions on Electron Devices, 1–8

Jayanthi, K., Chawla, S., Joshi, A.G., Khan, Z.H. and Kotnala, RK. 2010. "Fabrication of luminescent, magnetic hollow core nanospheres and nanotubes of Cr-doped ZnO by inclusive coprecipitation method", J Phys Chem C, 114, 18429–34.

Jung, E. Y., Park, C.-S., Hong, T. E., & Sohn, S. H. (2014). Effects of Sc- and Zr-doped MgO layers on electron emission and discharge characteristics of alternating-current plasma display panels. Japanese Journal of Applied Physics, 53(3), 036002.

Kadari, A. Mostefa, R., Khaled, M., Badaoui M., and Mebarek M. 2016. "Optical and structural properties of Mn doped MgO powders synthesized by Sol-gel process", Optik, 127(20), 8253-8258.

Khan, T.M., Iqbal, A. and Zakria, M. 2014. "Study of excitonic UV emission stability, green luminescence and bandgap tune-ability in wurtzite (ZnO)1− x (Cr2O3)x composite", Vacuum, 105,1–6.

Li, M.-J., Sun, J., Li, H.-J., Huang, B.-K., & Yang, B.-H. (2012). Effects of the Concentration of MgO in the Catalyst on the Growth of Carbon Nanotubes. Molecular Crystals and Liquid Crystals, 569(1),

Liu, H., Lu, H., Zhang, L., & Wang, Z. (2015). Orientation selection in MgO thin films prepared by ion-beam-deposition without oxygen gas present. Nuclear Instruments and Methods in Physics Research Section B: Beam Interactions with Materials and Atoms, 360, 60–63.

Maiti, P., Das, P.S., Bhattacharya, M., Mukherjee, S., Saha, B., Mullick, A.K.,

Mukhopadhyay, A.K. 2017. "Transparent Al+3 doped MgO thin films for functional applications", Mater. Res. Express, 4(8), 086405.

Mishra, D. Mandal, B.P. Mukherjee, R. Naik, R. Lawes, G. and Nadgorny, B. 2013. "Oxygen vacancy enhanced room temperature magnetism in Al-doped MgO nanoparticles", Appl. Phys. Lett., 102, 182404.

Płóciennik, P., Guichaoua, D., Zawadzka, A., Korcala, A., Strzelecki, J., Trzaska, P., & Sahraoui, B. (2016). Optical properties of MgO thin films grown by laser ablation technique. Optical and Quantum Electronics, 48(5)

Qi, L., Liu, L., Feng, S., Sun, H., & Han, R. (2017). Synthesis and magnetic properties of ceramic MgO porous film. Journal of the European Ceramic Society, 37(15), 4727–4731.

Rao, K. V. and Sunandana, C. S. 2008. "Structure and micro structure of combustion synthesized MgO nanoparticles and nanocrystalline MgO thin films synthesized by solution growth route", Synthesis and Reactivity in Inorganic, Metal-Organic and Nano-Metal Chemistry, 38(2), 173-180.

Shkir M., Anis M., Shafik S., Manthrammel M. A., Sayeed M.A., Hamdy M.S., AlFaify S. 2020. "An effect of Zn content doping on opto-third order nonlinear characteristics of nanostructured CdS thin films fabricated through spray pyrolysis for optoelectronics", Physica E, 118, 113955.

Xu, C., Cao, L., Su, G., Liu, W., Qu, X. and Yu, Y. 2010. "Preparation, characterization and photocatalytic activity of Co-doped ZnO powders", J Alloys Compd, 497,373–6.

Valanarasu, S., Dhanasekaran, V., Karunakaran, M., Vijayan, T. A., Chandramohan, R., & Mahalingam, T. (2014). Microstructural, optical and electrical properties of various time annealed spin coated MgO thin films. Journal of Materials Science: Materials in Electronics, 25(9),

Visweswaran, S., Venkatachalapathy, R., Haris, M., & Murugesan, R. (2020). Characterization of MgO thin film prepared by spray pyrolysis technique using perfume atomizer. Journal of Materials Science: Materials in Electronics.

Yu, H. K. 2018. "Secondary electron emission properties of Zn-doped MgO thin films grown via electron-beam evaporation", Thin Solid Films, 653, 57-61.